DETECTING THE CHANGES OF FENHE RIVER CHANNEL BY UNMIXING LANDSAT IMAGERY

Xin CAO[1], Weihua FANG[2,3,*], and Hidefumi IMURA[4]

[1]Doctoral Student, Graduate School of Environmental Studies, Nagoya University
(Furo-cho, Chikusa-ku, Nagoya, 464-8603, Japan)
[2]Assistant Professor, Key Lab of Environment Change and Natural Disaster, Ministry of Education of China,
(No. 19, Xinjiekouwai Street, 100875, China)
[3] Researcher, CREST, Japan Science and Technology Agency
E-mail: weihua.fang@gmail.com
[4]Member of JSCE, Professor, Graduate School of Environmental Studies, Nagoya University
(Furo-cho, Chikusa-ku, Nagoya, 464-8603, Japan)

Fenhe River (FR) basin in China has been suffering from water shortage, and FR began to experience dry-up from the early 1980s. Due to the lack of hydrological observations or poor quality of gauged record, it is difficult to understand its hydrological process. In this study, the river channel width (*CW*) and weighted river width (*WRW*) of the FR in 1976, 1990, 2000 and 2004 were defined and extracted through linear-unmixing of MSS, TM and ETM+ data of satellite Landsat. The results were proved by man-made dam and reservoir, but quantitative validation need accurate measurements in situ. The method has the potential to provide proxy information for poorly gauged basin.

Key Words : *Fenhe river channel, linear unmixing, weighted river width, Landsat*

1. INTRODUCTION

A variety of efforts had been made for modelling hydrological cycle and water resources in ungauged or poorly gauged basins in the past study[1,2]. Model validation or calibration may encounter difficulties due to inadequate or lack of runoff records. It is important to explore proxy data to substitute runoff gauge records[3]. Also, hydrological gauge records are limited to specific spots whereas information of river channel like river width and runoff volume can help understand water resource distribution in 2-dimension space.

Fenhe River (FR) basin in China experienced severe water shortage in the past several decades. From the early 1980s in some parts of the FR channel dry-up happened for long time periods[4]. Some hydrological stations along the drying-up FR channel ceased or suspended observation because the runoff volume was small or zero.

Satellite remote sensing can provide unique information on areas lacking of direct surface observation. Generally traditional classification of remotely sensed images regards one pixel as one land use or land cover type, although the pixel may actually be the mixture of several types. If river channel is detected only by classifying 28.5-meter or resampled 57-meter pixels Landsat images, river channel width could be heavily over or under estimated. Therefore a more accurate method is needed to extract finer or sub-pixel information to reflect the subtle changes of river channel.

Linear unmixing, also known as spectral mixture analysis (SMA), assumes the spectrum measured by a sensor is a linear combination of the spectra of all components, referred to as endmember, within one pixel[5,6]. The essential assumptions for linear

*Corresponding author.

unmixing are: 1) the landscape is composed of a few spectrally distinctive fundamental endmembers; 2) the spectral signature for each component is a constant within the entire spatial extent of analysis, and 3) the remotely sensed signal of a pixel is linearly related to the fractions of endmember present[7]. Linear unmixing was applied in a variety of studies, such as extracting crop distribution[8], classifying vegetation (especially sparse vegetation)[9,10,11], mapping floodplain habitats[12], determining urban land cover components[7,13], and estimating vegetation parameters[14].

For most rivers, water surface is the major component of a typical river channel. In the FR channel dry-up process frequently happened in the past 40 years. Therefore, beside water surface, river bed would emerge and vegetations like grass or shrub would appear in river bed in dry season and submerge in wet season.

The goals of this study are: 1) extracting the fracion of water surface within the FR channel, by linearly unmixing Landsat MSS (Multispectral Scanner), TM (Thematic Mapper) and ETM+ (Enhanced Thematic Mapper plus) imagery of 1976, 1990, 2000 and 2004, 2) defining and computing the FR channel width and river width, and 3) detecting the spatial and temporal changes of the FR channel.

2. DATA AND METHODS

(1) Data and Preprocess

The width of most of the FR channel ranges from 20 meters to 150 meters. In this study, Landsat images with 57 meters or 28.5 meters pixel sizes were selected to detect the changes of FR channel. The descriptions of acquired dates, sensors, spatial resolutions and bands of the Landsat imagery used in this study are listed in Table 1.

Prior to linear unmixing, the four images were geo-registered in UTM projection and the relative geometric errors were no more than one pixel. The DN (digital number) values of raw data were converted into radiance with unit of $Watt \cdot m^{-2} \cdot sr^{-1} \cdot \mu m^{-1}$ [15,16]. The radiance were then atmospherically corrected and converted into unitless surface reflectance using 6S model[17].

Besides the above Landsat imagery, a river polyline was manually digitized in geographic information system (GIS) based on remotely sensed images. A polygon buffer was then created with a side distance of 300-meter vertical to river line. The polygon with the width of 600-meter can cover all of the FR channel. The total length of the polygon is approximate 265 km (Fig. 1).

Table 1 The parameters of the 4 Landsat imagery

Satellite	Landsat-2	Landsat-5	Landsat-7
Sensor	MSS	TM	ETM+
Date	1976/06/25	1990/09/16	2000/07/01 2004/04/15
Pixel size (m)	57	28.5	28.5
Bands (μm)	B4(0.5-0.6) B5(0.6-0.7) B6(0.7-0.8) B7(0.8-1.1)	B1(0.45-0.52) B2(0.52-0.60) B3(0.63-0.69) B4(0.76-0.90) B5(1.55-1.75) B7(2.08-2.35)	B1(0.45-0.52) B2(0.53-0.61) B3(0.63-0.69) B4(0.78-0.90) B5(1.55-1.75) B7(2.09-2.35)

(2) Linear Unmixing

The basic function of linear unmixing is

$$P'_{i\lambda} = \sum_{k=1}^{N} f_{ki} \times P_{k\lambda} + \varepsilon_{i\lambda} \qquad (1)$$

where $P'_{i\lambda}$ is the measured spectral mixture from location i. $P'_{i\lambda}$ is modeled as the sum of k-th endmembers, $P_{k\lambda}$, weighted by fraction f_{ki}. N is total number of endmembers. Unmodeled portions of the spectrum are expressed as a residual term, $\varepsilon_{i\lambda}$, at wavelength λ.

In this study, fractions were constrained by

$$\sum_{k=1}^{N} f_{ki} = 1.0 \quad \text{and} \quad 0 \le f_{ki} \le 1.0 \qquad (2)$$

The endmember may be selected from image (image endmember) or derived from a library or field reflectance spectra (reference endmember) [6]. In order to select endmembers from images, the Principal Components (PCs) were computed by

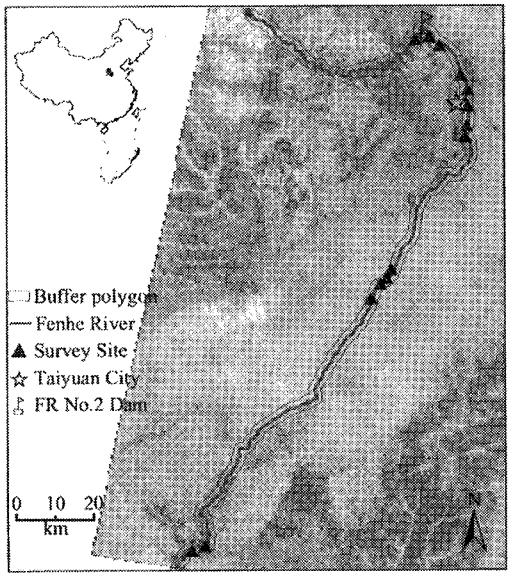

Fig. 1 River channel, buffer polygon and survey sites along the Fenhe River (FR).

Principal Component Analysis (PCA). For the four images in this study, the first several PCs contains almost all variances of multispectral images, therefore the endmembers can be selected from scattering plot of these PCs[18].In order to reflect the changes within the drying-up FR channel, water, soil and vegetation were chosen as the endmembers.

The eigenvalues of PCs of the 4 Landsat images in this study were listed in Table 2. For the above 4 images the variances of their first and second PCs are all approximate 99%, i.e., these two PCs contain most of the information of the images. Fig. 2 is an example of scatter plots from first and second PCs, from which the endmembers of water, soil and vegetation were selected.

The linear unmixing assumes that the spectral characteristic of each endmember is unique and constant. However, the image endmember may contain inherent spectral variances when many pixels are assigned to one endmember. A simple method to eliminate the variability of endmembers named as normalization method[13] was proposed as

$$\overline{R_b} = 100 \times R_b \Big/ \left(\frac{1}{N} \sum_{b=1}^{N} R_b \right) \qquad (3)$$

where $\overline{R_b}$ is normalized reflectance for band b, R_b is the original reflectance for band b, and N is the total number of bands. The normalized spectra of three endmembers were shown in Fig. 3.

The fraction of each endmember was calculated by solving function (1) with function (2) as constraint, using the mean normalized reflectances and least square method.

(3) Definition of channel width (*CW*) and weighted river width (*WRW*)

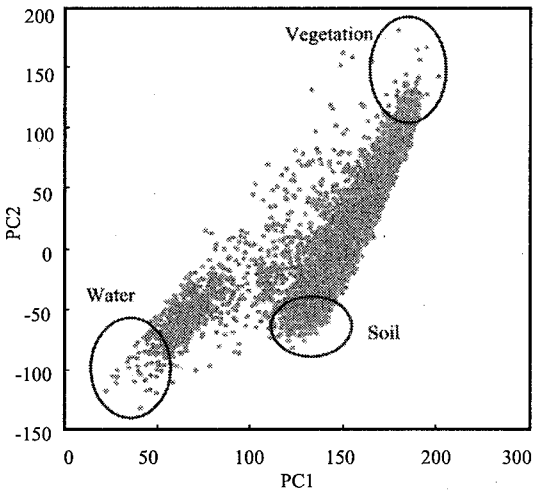

Fig. 2 An example of scattering plot (feather spaces) of the first and second PC components with ETM+ data (2000/07/01).

Table 2 Eigenvalues of principle components

Data	PC	Eigenvalue	Normalized
MSS (1976/06/25)	1	13006.6	0.936
	2	858.6	0.062
	3	15.5	0.001
	4	8.9	0.001
TM (1990/09/16)	1	24503.4	0.940
	2	1351.0	0.052
	3	157.1	0.006
	4	29.2	0.001
	5	16.3	0.001
	6	8.3	0.000
ETM+ (2000/07/01)	1	18033.1	0.928
	2	1208.3	0.062
	3	145.8	0.008
	4	16.8	0.001
	5	14.3	0.001
	6	4.1	0.000
ETM+ (2004/04/15)	1	2457.7	0.989
	2	18.1	0.007
	3	8.3	0.003
	4	1.4	0.001
	5	0.6	0.000
	6	0.0	0.000

Conventionally, the width of river is regarded as the distance between two banks, it is always constant and not related to the runoff. However, the width of water surface is fluctuated and runoff related. Two

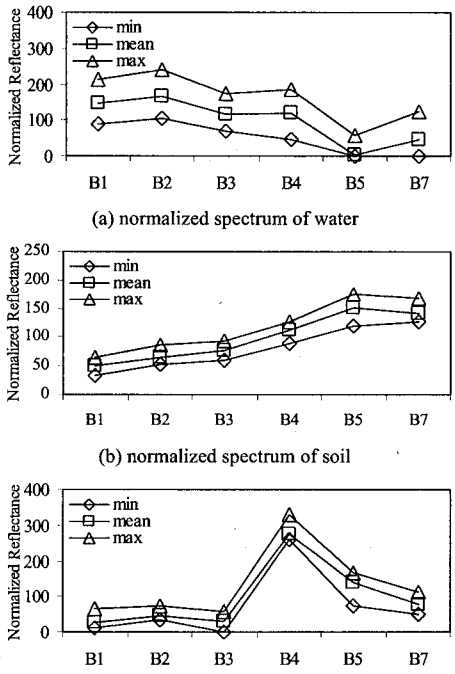

Fig. 3 Nnormalized spectra of water-soil-vegetation endmember components derived from ETM+ data (2000/07/01).

concepts of width were proposed here: channel width (*CW*) and weighted river width (*WRW*) based on fraction of water by linear unmixing.

Firstly, river channel was defined as the pixels inside the 600-meter polygon, whose water fraction are equal to or larger than a threshold of 0.2. The threshold was decided according to field survey knowledge and visual effect inspection of unmixed water component. These pixels could be regarded as classified river channel pixels by traditional classification method.

Supposing there are m pixels in the insection of an ideally straight river channel (Fig. 4a), the *CW* is calculated as

$$CW^{Straight} = P \times n \tag{4}$$

where P is the size of pixel, n is the number of pixels equel to or larger than threshold 0.2. Similarly, the water area fraction derived from linear unmixing in pixel i ($i=1,2,\ m$) is f_i, then *WRW* is defined as

$$WRW^{Straight} = P \times \sum_{i=1}^{m} f_i \tag{5}$$

However, the actual FR channel is not an ideally straight line but a curve (Fig. 4b) wandering from Luliang Mountain to Fenhe Plain. In order to convert the smooth river curve into a straight line, the 265km FR channel was disassembled into 530 500m-length piece buffers (shadow area in Fig. 4b), whose area (A) were accessed by spatial analysis in ArcGIS™. The buffer of piece was then converted into an equal area rectangle with 600m width. In this way *WRW* is calculated as

$$WRW = \frac{\sum_{i=1}^{m} f_i \times s}{A/600} \tag{6}$$

where *WRW* is mean water fraction weighted river width of each piece, s is the image pixel area, $A/600$ is the length of rectangle. The *CW* is calculated by the same way but replace $\sum_{i=1}^{m} f_i$ with n

$$CW = \frac{n \times s}{A/600} \tag{7}$$

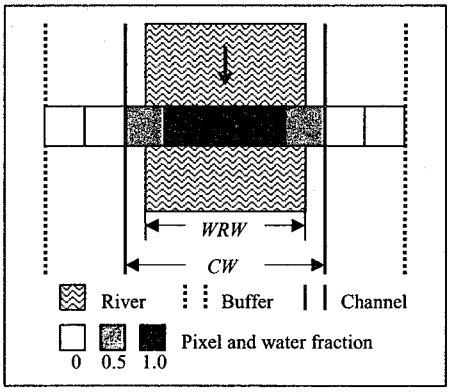

(a) ideally straight river channel

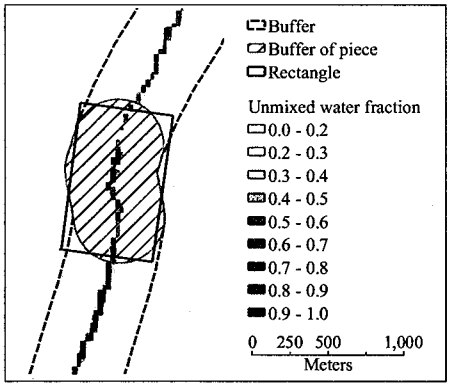

(b) curve river channel

Fig. 4 The illustration of channel width (*CW*) and weighted river width (*WRW*) calculation.

3. RESULTS

The *CW* and *WRW* of FR channel of 1976, 1990, 2000 and 2004 are shown in Fig. 5 .

(1) Spatial characteristics along the FR channel

The *WRW* of 1976 has a wider middle stream but comparablely narrow upper stream and down stream. In 1990 the *WRW* varies little since it has the most narrow *WRW* among all 4 years. For 2000 and 2004, the *WRWs* of FR vary greatly from upper stream to downstream.

(2) Temporal change of the FR channel

The general changing trend of both *CW* and *WRW* are decreasing. The average *CW* and *WRW* of the whole detected river channel in the June, 25th of 1976 were 169.3 and 82.8 meters respectively. As to the same period (July 1st) of the year of 2000, *CW* and *WRW* were only 82.9 and 37.1 meters, which were significantly narrower than that of 1976.

For the year of 2004 in April, the values were 44.7 and 36.2 meters. In the September of 1990, *CW* and *WRW* were 41.9 and 16.0 meters.

Although it must be cautious of comparing *CW* and *WRW* in different seasons of different years due to inter-annual climate fluctuation, an obvious decrease of *CW* and *WRW* is shown in Fig. 5.

(3) Validatation

Due to the lack of runoff and hydrological data, the validation of the result relies greatly on field survey. Two field surveys were carried out in February and September of 2005 respectively. The two survey routes ranges from NO.2 FR Dam to the intersection

of the FR downstream and the Yellow river main stream with car-borne GPS to provide surveying positions (Fig. 1). However, the measurement of width is difficult, and the estimation of water fraction in one coordinated pixel is also troublesome. Thus the validation is carried out by the comparison between the situations before and after the construction of NO.2 FR dam, and the formation of reservoir in Taiyuan city.

NO.2 FR dam was constructed from November of 1996, and began to operate in April, 2000. The *WRW* results of 2000 (Fig.5c) and 2004 (Fig.5d) show the location of the NO.2 FR dam and reservoir in Taiyuan City. The Wanjiazhai Project transferred water from the Yellow river to Fenhe river since Oct., 2003, which led to an increment of river width in 2004 at No. 2 FR dam and the formation of artificial reservoir in Taiyuan City (100-110km). Fig. 6 shows two photos taken in Taiyuan City in February 2005. Fig. 6 (a) is the artificial reservoir in north of the bridge (seen in Fig. 6b), Fig. 6 (b) is the dry river channel in south of the bridge. These two photos indicate the sudden switch of river width (*WRW*) in Taiyuan City.

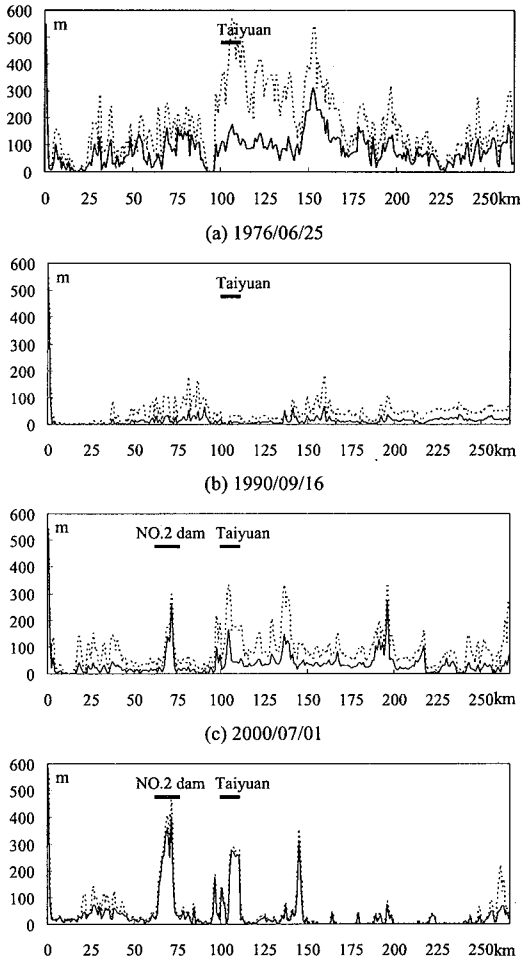

(a) 1976/06/25

(b) 1990/09/16

(c) 2000/07/01

(d) 2004/04/15

Fig. 5 Channel width (*CW*, dashed) and weighted river width (*WRW*, solid line) of FR by linear unmixing of Landsat images (1976, 1990, 2000 and 2004)

4. DISCUSSION

(1) Limitations of linear unmixing

Although normalized method could reduce spectral fluctuate in some extent, the unmixed water component still has inherent errors introduced by remained spectral instability of endmembers (Fig. 3, noticing the maximum and minimum reflectances). The upper stream of the FR is located in the valley of mountainous area and hence there are some shadow areas. In the Taiyuan city, some impervious areas are near to the FR channel. The spectrum of shadow and some impervious areas in Landsat bands are similar to that of water surface. Therefore the above areas have the possibility of being wrongly unmixed as water surface. Additional efforts should be implemented. For example, field survey knowledge and digital elevation model (DEM) were utilized to eliminate those non-water pixels with low albedo.

(2) Results and validation

The remotely sensed data of 1976, 1990, 2000 and 2004 were all daily images, i.e., they presented the daily situations but not the average annual runoff or river width. The daily runoff may vary greatly. Due to the lack of measured runoff and river width data,

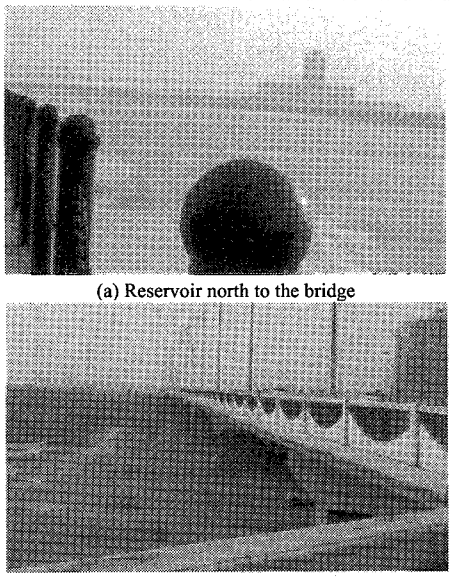

(a) Reservoir north to the bridge

(b) Dry river channel south to the bridge

Fig. 6 Photos of FR channel in Taiyuan City (February, 2005)

the validation of the results was not rigorous. However, the existence of NO. 2 FR dam and reservoir in Taiyuan City provided the relatively convincing evidences for the method.

5. Conclusion

This study proposed a method to estimate river channel width and river surface width, termed *CW* and *WRW*, using satellite remotely sensed data, linear unmixing technology and GIS analysis. The results illustrated the significant variations along FR channel during 1976-2004. Although the results were not fully quantificationally validated, the NO. 2 FR dam and reservoir in Taiyuan City were successfully detected. The method has the potential to provide proxy hydrological information in poorly gauged area. Further studies are needed to improve and consolidate validation.

ACKNOWLEDGMENT: Financial assistance for this work was provided by the CREST of Japan Science and Technology Corporation under the project "Sustainable development and management for water resources in the Yellow River basin".

REFERENCES

1) Yang, D., Kanae, G. Ni, S., LI, C. and Kusuda, T.: Water resources variability from the past to future in the Yellow River of China, IAHS publication, 295, 174-182, 2005.
2) Fang, W. H., and IMURA, H.: The spatial and temporal changes of pan evaporation from 1971 to 2000 in the Yellow River basin, *Environmental Systems Research*, 33: 165-170, 2005.
3) Fan D. X. (editor): *Water resources assessment for Shanxi province*, Beijing: China WaterPower Press, 2005.
4) IPCC: Climate change: *The scientific basis*, Cambridge university press, 2001.
5) Shimabukuro, Y. E., and Smith, J. A.: The least squares mixing models to generate fraction images derived from remote sensing multispectral data, *IEEE Transactions on Geoscience and Remote Sensing*, 29: 16-20, 1991.
6) Adams, J. B., Smith, M. O., and Gillespie, A. R.: Imaging spectroscopy: Interpretation based on spectral mixture analysis. In C. M. Pieters, & P. A. J. Englert (Eds.), Remote geochemical analysis: Elemental and mineralogical composition. Cambridge, England: Press Syndicate of University of Cambridge, pp. 145-166, 1993.
7) Song, C.: Spectral mixture analysis for subpixel vegetation fraction in the urban environment: How to incorporate endmember variability? *Remote Sensing of Environment*, 95: 248-263, 2005.
8) Lobell, D. B., and Asner, G. P.: Cropland distributions from temporal unmixing of MODIS data, *Remote Sensing of Environment*, 93 (3): 412-422, 2004.
9) DeFries, R. S., Hansen, M. C., and Townshend, J. R. G.: Global continuous fields of vegetation characteristics: A linear mixture model applied to multi-year 8 km AVHRR data, *International Journal of Remote Sensing*, 21: 1389-1414, 2000.
10) Braswell, B. H., Hagen, S. C., Frolking, S. E., and Salas, W. A.: A multivariable approach for mapping sub-pixel land cover distributions using MISR and MODIS: Application in the Brazilian Amazon region, *Remote Sensing of Environment*, 87 (2-3): 243-256, 2003.
11) Sohn, Y., and McCoy, R. M.: Mapping desert shrub rangeland using spectral unmixture and modeling spectral mixtures with TM data, *Photogrammetric Engineering and Remote Sensing*, 63: 707-716, 1997.
12) Novo, E. M., and Shimabukuro, Y. E.: Identification and mapping of the Amazon habitats using a mixing model, *International Journal of Remote Sensing*, 18: 663-670, 1997.
13) Wu, C.: Normalized spectral mixture analysis for monitoring urban composition using ETM+ imagery, *Remote Sensing of Environment*, 93: 480-492, 2004.
14) Gilabert, M. A., Garcia-Haro, F. J., and Melia, J.: A mixture modeling approach to estimate vegetation parameters for heterogeneous canopies in remote sensing, *Remote Sensing of Environment*, 72: 328-345, 2000.
15) Markham, B. L., and Barker, J. L.: Radiometric properties of U.S. processed Landsat MSS data, *Remote Sensing of Environment*, 22: 39-71, 1987.
16) Chander, G., and Markham, B.: Revised Landsat-5 TM radiometric calibration procedures and postcalibration dynamic ranges. *IEEE Transactions on Geoscience and Remote Sensing*, 41 (11): 2674-2677, 2003.
17) Vermote, E. F., Tanré, D., Deuze, J. L., Herman, M., and Morcrette, J. J.: Second Simulation of the SatelliteSignal in the Solar Spectrum (6S), 6S User's Guide Version 2, NSAS Goddard Space Flight Center, Code 923, Greenbelt, MD, 1997.
18) Bateson, A., and Curtiss, B.: A method for manual endmember selection and spectral unmixing, *Remote Sensing of Environment*, 55: 229-243, 1996.

Landsat画像データによる河川水域の検出：中国フン河流域を対象に

曹　鑫・方　偉華・井村　秀文

フン河流域は水量の不足が続いており、1980年代前半にからは断流現象も始まっている。しかし、水文データや観測データの不足から、水循環のプロセスを解明することが困難である。本研究では、Landsatによるデータにlinear-unmixingを行い、1976年、1990年、2000年、2004年についてのフン河の河床、川幅channel width(*CW*)、水域率weighted-river width (*WRW*)を定義し、抽出した。また、フン河川水域の変化を分析した。この方法は観測データの乏しい流域に対する代替データとして有用である。